Hindawi
Journal of Nanomaterials
Volume 2023, Article ID 2508422, 9 pages
https://doi.org/10.1155/2023/2508422

Research Article

Prediction of CI Engine Emissions Fueled with Multiwalled Carbon Nanotube-Doped Waste Cooking Oil Biodiesel using Multilayer Neural Network

Syed Sameer Hussain,[1] Syed Abbas Ali,[1] Altaf Hussain Bagwan,[1] Dilawar Husain,[2] and Akbar Ahmad[3]

[1]*Department of Mechanical Engineering, SECAB Institute of Engineering and Technology, Vijaypur, India*
[2]*Department of Mechanical Engineering, Maulana Mukhtar Ahmad Nadvi Technical Campus, Mansoora, Malegaon, Nashik 423203, India*
[3]*Faculty of Science and Information Technology, MI College, Malé 20260, Maldives*

Correspondence should be addressed to Akbar Ahmad; akbar@micollege.edu.mv

Received 14 September 2022; Revised 19 November 2022; Accepted 26 November 2022; Published 16 January 2023

Academic Editor: Ümit Ağbulut

Nanocatalysts play a significant role to improve the thermal and physical properties of biodiesel. In the present work, the multiwalled carbon nanotubes (MWCNTs) as an additive with the fraction of 30, 40, and 50 ppm are dispersed with the different biodiesel–diesel blends of 10%, 30%, and 50% of waste cooking oil (WCO)-based biodiesel (B10, B30, B50) for the prediction of four-stroke compression ignition (CI) engine emissions using multilayer neural network (MLNN) model. An MLNN model uses a backpropagation algorithm to map input and output parameters. The input parameters to MLNN are load, blends, and MWCNTs in ppm. On the other hand, the output parameters are HC, CO, and NO_x. The results for the optimum topological structure of 3-10-3 denoted mean square error (MSE) equal to 0.095 that are capable of predicting the emissions for different operating conditions. Thereafter, the developed MLNN model is tested on an experimental setup consisting of a single-cylinder four-stroke CI engine and emission analyzer. The emission characteristics predicted by MLNN are called to be nearly experimental measurements with reasonable accuracy as it depicts the good "R" values as 0.95, 0.96, and 0.976 for HC, CO, and NO_x, respectively, and also gives the reasonable average relative error values as 0.83%, 1.01%, and 1.05%, for HC, CO, and NO_x, respectively. Further, the developed model is suitable for predicting emissions of CI engines, thus minimizing the cost, time, and labor effort.

1. Introduction

The research on alternative fuels has received attention due to growing demand and limited availability of petroleum; the cost is rising. Because of that, there is a requirement to search for alternate fuels for compression ignition (CI) engines [1]. In this connection, biodiesel from nonedible oils as feedstock becomes of greater interest. However, the cost associated with the production is high as compared with diesel. Due to the aforesaid reason, biodiesel is not appropriate for commercialization. In this context, there is a need for biodiesel whose production cost should be less compared with diesel. Further, waste cooking oil (WCO) is considered an economical biodiesel feedstock as its price is considerably lower than oil from other sources [2–5]. In the previous works, investigation of CI-engine parameters has been carried out via experiments [5–8]. Further, in recent advances, nanotechnology proved that nanomaterial-dispersed fuel can be used for better performance of engines due to its good mechanical and thermophysical properties than traditional materials [9–13]. The research work related to the experimentation of CeO_2 [14] and ZnO_2 [15] influence on CI engine operated with biodiesel is observed. Experimental discussion on the influence of carbon nanotubes over the diesel engine is reported by Tewari et al. [16] and by Basha and Anand [17], the result of Al_2O_3 and CeO_2 added in

Figure 1: Dispersion of nanoparticles with biodiesel.

biodiesel (Jatropha) is given in a study by Prabhu [18], and the influence of various concentrations of magnesium oxide in WCO-based biodiesel is appeared in a study by Ranjan et al. [19]. Even so, testing of engine for all operating conditions needs more money and time. As an alternative, the numerical/mathematical approach and neural network (NN) approach can be put to use for the investigation of engine variables associated with thermos-physical properties, performance, and emissions [20–25]. However, computational complexity limits the use of mathematical models. Alternatively, NN can be exploited for the same as it is advantageous over other techniques, viz., generalization capability, huge data-handling ability, mapping ability, etc. [20–25]. A NN model based on a backpropagation algorithm is utilized to determine the parameters/variables of the engine operated with blended biodiesel that has appeared in a study by Yusaf et al. [22]. Additionally, several studies [23–26] emphasized on the investigation of emission constituents and performance of engines operating on diesel, biodiesel, and nanoadditives biodiesel through the artificial NN. The metallic and carbon nanotubes (CNTs) become advantageous concerning emission reduction and have remarkable mechanical properties [16]. As far as the authors' knowledge, limited work has highlighted the impact of multiwalled carbon nanotubes (MWCNTs) on WCO biodiesel in diesel engines. Further, the gap in the literature on engine emissions while adding CNTs to biodiesel fuel appears to be addressed. Furthermore, the ability of NN to predict emissions of engine runs on low-cost biodiesel (WCO) dispersed with MWCNTs has yet to be investigated in the previous works. Subsequently, this work has been implemented to fill the gap available in the literature. Keeping this concept in the mind, a multilayer NN has been constructed to predict the emissions, viz., HC, CO, and nitrogen oxides (NO_x) from the CI engine run on WCO as biodiesel dispersed with MWCNTs.

2. Experimental Procedure, Setup, and Investigations

2.1. Experimental Procedure. The study involves the preparation of biodiesel using WCO as feedstock, and then different blends (10%, 30%, and 50%) of WCO-based biodiesel (B10, B30, B50) and diesel have been prepared. Further, the dispersion of MWCNTs is carried out with the different dosing levels of 30, 40, and 50 ppm in WCO blends through ultrasonicator (Figure 1), which mixes the nanoparticles into the diesel+WCO biodiesel fuel, as it helps agglomerate particles' restoration to nanometer range. The resulted MWCNTs-blended WCO biodiesel is placed in beaker under static condition to assure the stability. Further, the MWCNTs are obtained from "Platonic Nanotech Private Limited," Mahagama, India. Further, some of the properties of MWCNTs are shown in Table 1. Thereafter, the scanning electron microscope (SEM) picture is shown in Figure 2 and transmission electron microscope (TEM) picture is shown in Figure 3. As shown in Figures 2 and 3, it is revealed that CNTs material are having tube-like structure and the width of 4–22 nm and length of about 60–150 nm. Figure 4 represents X-ray diffraction (XRD) pattern of MWCNTs, and they are not crystalline in nature.

Table 1: Properties of multiwalled carbon nanotubes.

S. No.	Particulars	Range/value
1.	Electric conductivity	10^8 S/m
2.	Modulus	7 time metal
3.	Thermal conductivity	6×10^3 W/mK
4.	Tensile strength	30–80 GPa

Figure 2: SEM picture of MWCNTs.

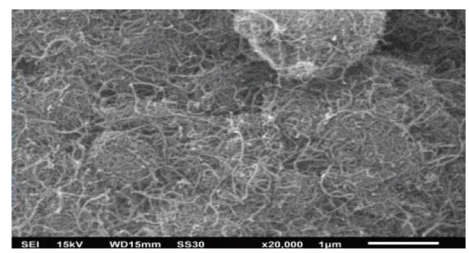

Figure 3: TEM picture of MWCNTs.

2.2. Properties of Pure Diesel and WCO Biodiesel Blends with MWCNTs. Testing of the prepared samples dispersed with MWCNTs has been carried out to obtain the values of density in kg/m^3, viscosity in cSt, calorific value in kJ/kg, and flash and fire point in °C. Further, the properties of pure diesel and WCO biodiesel blends with MWCNTs for 30, 40, and 50 ppm are shown in Tables 2–4, respectively.

2.3. Engine Setup. The direct injection (DI), four-stroke single cylinder CI engine is shown in Figure 5 and its instrumentation part is shown in Figure 6(a). It comprises of a bed, engine connected to eddy dynamometer. The dynamometer has been used to load the engine. To circulate the water to the calorimeter and dynamometer, pump is provided. A tank for fuel is placed into control panel accompanied by fuel unit for measurement. The test engine runs at steady speed of

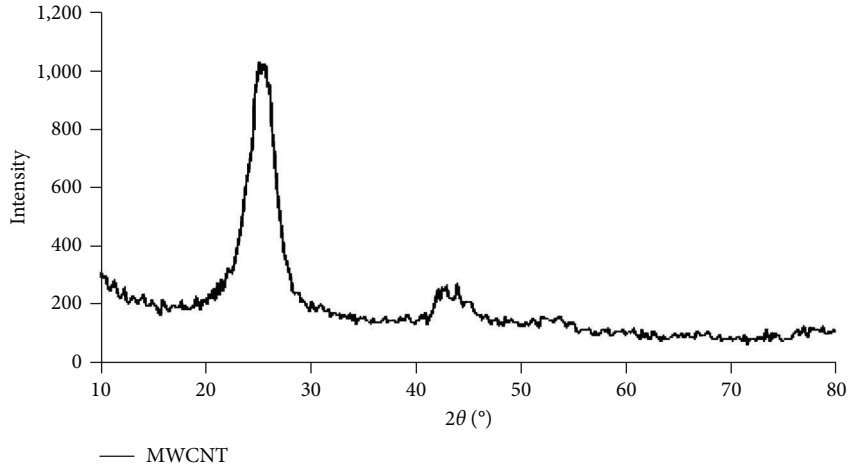

Figure 4: XRD analysis of MWCNTs.

Table 2: Properties of pure diesel and WCO biodiesel blends with MWCNTs (30 ppm).

S. No.	Particulars	Pure diesel (B0)	WCO biodiesel +MWCNTs		
			B10	B30	B50
1.	Calorific value	44,000	42,700	41,541	40,100
2.	Density	832	799	838	860
3.	Viscosity	2.27	2.8	3.87	4.9
4.	Flashpoint	69	52	96.8	105.4
5.	Firepoint	53.4	58	100.9	129.2

Table 3: Properties of pure diesel and WCO biodiesel blends with MWCNTs (40 ppm).

S. No.	Particulars	Pure diesel (B0)	WCO biodiesel +MWCNTs		
			B10	B30	B50
1.	Calorific value	44,000	42,800	40,955	40,000
2.	Density	832	800	848	870
3.	Viscosity	2.27	2.7	3.7	5.2
4.	Flashpoint	69	60	90	107
5.	Firepoint	53.4	63	98	119

1,500 rpm at rated power, which make use of B10, B30, and B50 blends. The emission characteristics for each test condition and blend are measured using emission analyzer, as shown in Figure 6(b). The fuel tank is made completely empty for every time, and then new WCO-blend-dispersed MWCNTs are poured into tank and engine emissions are measured. Further, the specification of engine and emission analyzer is shown in Tables 5 and 6, respectively.

2.4. Uncertainty Analysis. Uncertainty analysis of the various parameters has been carried out to overcome the errors involved in the instruments. The error and uncertainty of instruments depend upon the working and natural conditions and instrument's accuracy [25]. In this, tests are performed many a time and mean values are utilized for further analysis (Table 7).

Table 4: Properties of pure diesel and WCO biodiesel blends with MWCNTs (50 ppm).

S. No.	Particulars	Pure diesel (B0)	WCO biodiesel +MWCNTs		
			B10	B30	B50
1.	Calorific value	44,000	43,000	40,912	38,099
2.	Density	832	843	859	839
3.	Viscosity	2.27	2.6	3.88	5.0
4.	Flashpoint	69	66	87	101
5.	Firepoint	53.4	76	111	152

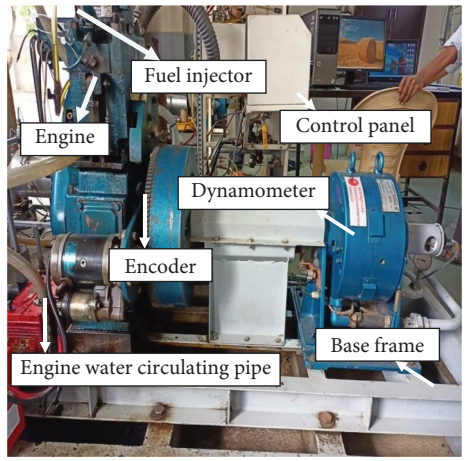

Figure 5: Four-stroke diesel engine setup.

2.5. Experimental Investigations of Emissions

2.5.1. Hydrocarbons. Figures 7–9 show the effect of hydrocarbons (HC) with respect to load for B0, B10, B30, and B50 mixed with MWCNTs of 30, 40, and 50 ppm, respectively. It is distinguished from Figures 7–9 that HC emissions are

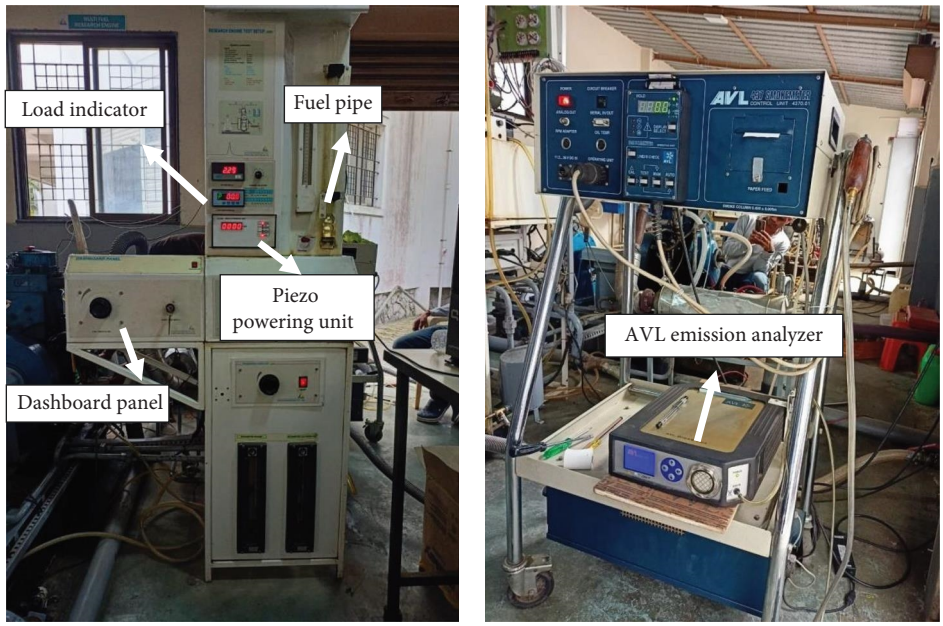

(a) (b)

Figure 6: Photograph of (a) instrumentation part; (b) emission analyzer.

Table 5: Some main specifications of engine.

Particulars	Specifications
Type of engine	Four stroke
Fuel used	Diesel
Type of cooling	Water cooled
Range of speed	1,200–1,800 rpm
Power	3.5 KW at 1,500 rpm
Displacement volume	661 cc
Bore of cylinder	87.5 mm
Stoke	110 mm
Compression ratio	12–18
Dynamometer	Eddy current with loading unit

Table 6: Charecteristics of emission analyzer.

Particulars	Measurement
Range of HC	0–20,000 ppm vol.
Range of CO	0%–15% vol.
NO_x	0–5,000 ppm vol.
CO_2	0%–20% vol.
O_2	0%–25% vol.
Display	LCD
Interface	USB
Operating voltage	100–300 VAC
Dimensions ($w \times h \times l$)	$270 \times 85 \times 320$ mm
Type	AVL DIGAS 444N

Table 7: Uncertainty analysis.

Particulars	Resolution
HC range	1 ppm
CO range	0.001% vol.
NO_x	1 ppm vol.
O_2	0.01% vol.
CO_2	0.1% vol.
Load indicator	0.2 bar
Crank angle sensor	1°

increasing with the increase in the load for all the blends; this is because, for small loads, fuel consumption is less, resulting in less emissions, whereas for higher loads, fuel consumption is high as a result of higher emissions [11, 13, 18]. HC emissions are diminished by applying 30, 40, and 50 ppm of MWCNTs. Nanoparticles act as oxidation catalysts, which improve the oxidation and, as a result, lower the HC emissions [13, 18]. This is due to increase in the surface-to-volume ratio and good fuel–air-mixing rate.

2.5.2. Carbon Monoxide. Figures 10–12 show the effect of carbon monoxide (CO) with load B0, B10, B30, and B50 mixed with MWCNTs of 30, 40, and 50 ppm, respectively. It is noticed from Figures 10–12 that the CO emissions are decreasing with the increase in the load for all the blends, this is due to improved combustion; it is also seen that CO emission for the WCO biodiesel mixed with MWCNTs is marginally less in comparison with that of B0. This is because the increasing content of oxygen with MWCNTs in the blends and higher surface-to-volume ratio of nanoparticles [13, 18].

2.5.3. Nitrogen Oxides. Figures 13–15 show the effect of NO_x with load B0, B10, B30, and B50 mixed with MWCNTs of 30, 40, and 50 ppm, respectively. It is noticed from Figures 13–15 that NO_x emissions are increasing with the increment in the load for all the blends; this is because of

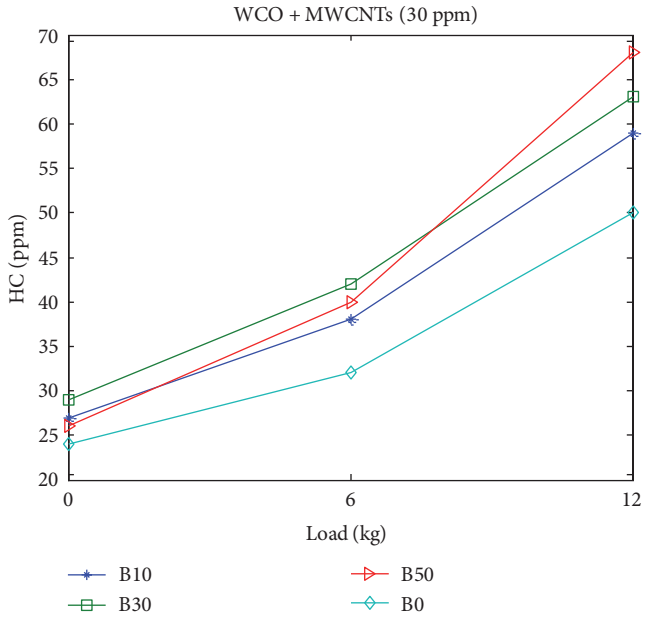

Figure 7: Effect of HC versus load for biodiesel mixed with MWCNTs (30 ppm).

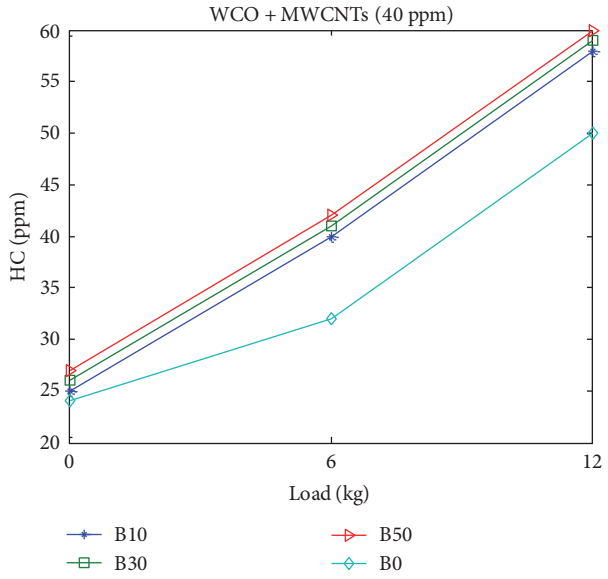

Figure 8: Effect of HC versus load for biodiesel mixed with MWCNTs (40 ppm).

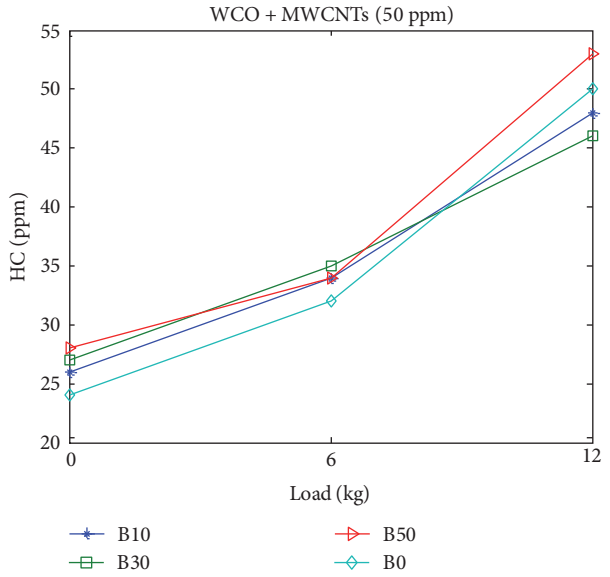

Figure 9: Effect of HC versus load for biodiesel mixed with MWCNTs (50 ppm).

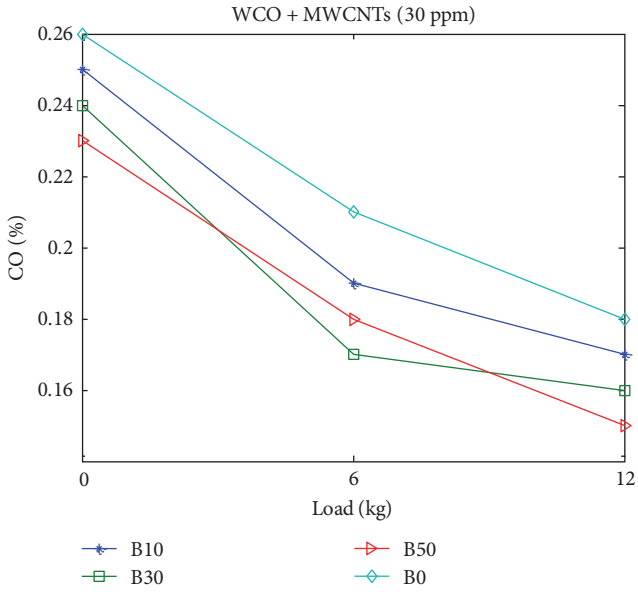

Figure 10: Effect of CO versus load for biodiesel mixed with MWCNTs (30 ppm).

improvement in combustible temperature, oxygen quantity in higher value, and fast reaction rate [27]. The addition of MWCNTs into fuel leads to complete combustion as it works as an oxygen-donating catalyst inside the combustion chamber [13, 18].

3. Multilayer Neural Network

In this work, the feed-forward backpropagation multilayer neural network (MLNN), as shown in Figure 16, is applied to map each parameter because it is called as universal approximator and highly appropriate for nonlinear plants [24, 25]. The superiority of MLNN compared with other approaches is that it could be utilized to model the nonlinear plant and can come up with input–output/target mapping, adaptive, and fault tolerance [28, 29]. MLNN is used to model the variables and the output/target is depicted by Equation (1).

$$E(w) = f[l_1, l_2, l_3, w], \tag{1}$$

where $E(w)$ is the target of MLNN. The tangent hyperbolic (tanh) function and linear function are utilized for unseen

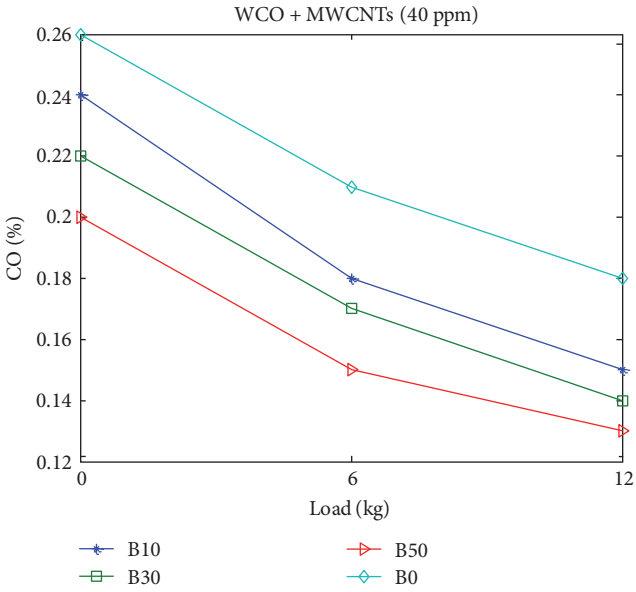

Figure 11: Effect of CO versus load for biodiesel mixed with MWCNTs (40 ppm).

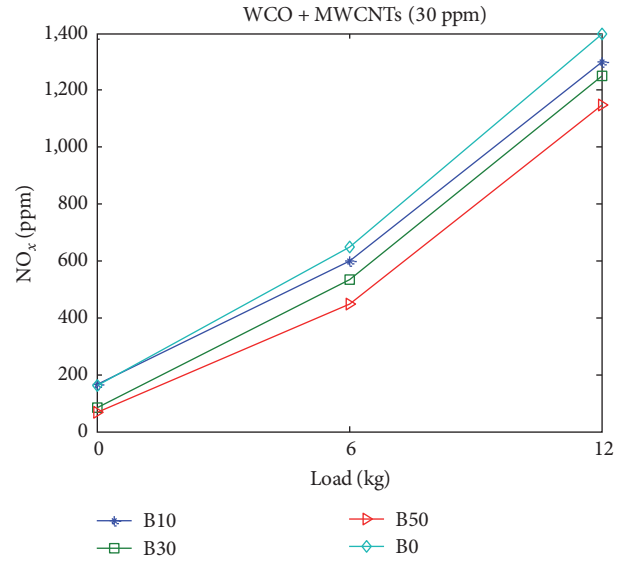

Figure 13: Effect of NO_x versus load for biodiesel mixed with MWCNTs (30 ppm).

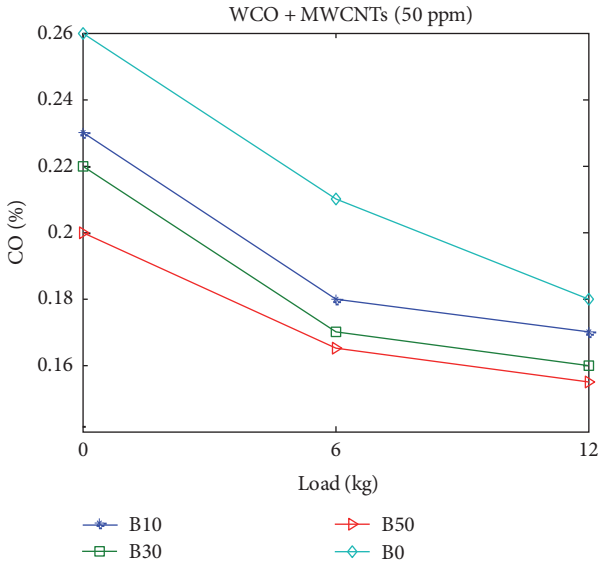

Figure 12: Effect of CO versus load for biodiesel mixed with MWCNTs (50 ppm).

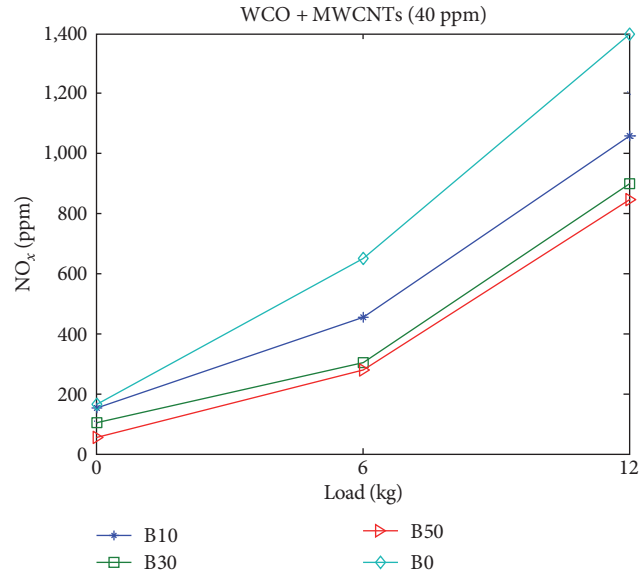

Figure 14: Effect of NO_x versus load for biodiesel mixed with MWCNTs (40 ppm).

(hidden) and output layers, using Equations (2) and (3), respectively [28, 29].

$$\phi_{\tanh}(i) = \tanh(i), \tag{2}$$

$$\phi_{\text{lin}}(i) = i. \tag{3}$$

In Equations (1)–(3), i is the input to the input neurons, w is the weight vector, to be calculated over the entire training process, and l_1, l_2, l_3 are the input variables to the network.

The engine load, WCO biodiesel blends, and MWCNTs ppm are the inputs to the MLNN. One can calculate the weights w by minimizing the cost function $\xi(w)$ defined by Equation (4).

$$\xi(w) = \frac{1}{2N_q} \times \sum \varepsilon \times (w)^2 + \frac{1}{N_q} \times w^T \times D \times w, \tag{4}$$

where $\varepsilon(w) = y - \hat{y}$ and the weight decay matrix is designated as D.

To acquire the outline, data points on the network structure are segregated into first subset 70%, second subset 15%, and third subset 15% of data. The first subset data are utilized for training process, whereas second and third subsets are used for validation and cross-validation (testing), respectively.

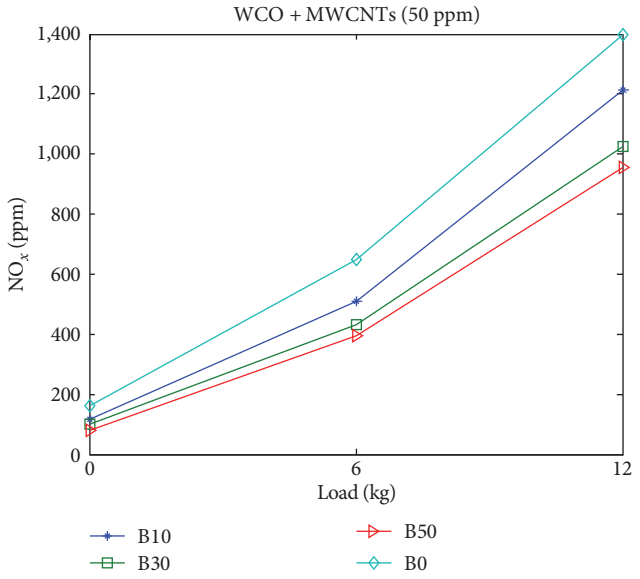

Figure 15: Effect of NO_x versus load for biodiesel mixed with MWCNTs (50 ppm).

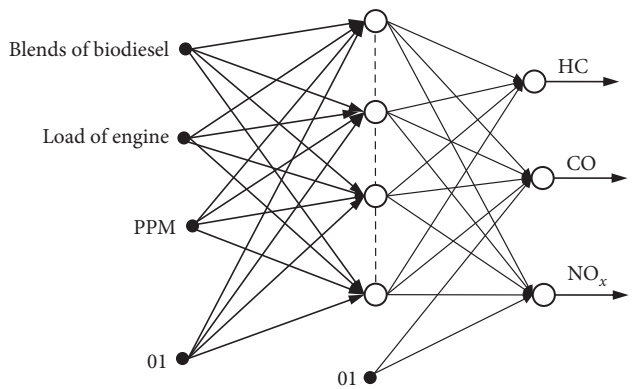

Figure 16: Structure of MLNN.

The best epoch can be selected by observing early stopping technique (Figure 17). Several MLNN architectures/topologies are trained by varying neuron numbers from 2 to 12 in hidden layer. For this, MATLAB® 2014(b) is used. The architecture/topology that describes the minimal mean square error (MSE) corresponds to validation data is opted as the optimum network to predict the target parameters. The validation data MSE for various topologies are given in Table 8. The optimum architectures seem to be suitable for predicting emissions over any test conditions of engine.

4. Results and Discussion

In this manuscript, the results acquired with MLNN predict the emissions of four-stroke CI engine operated on biodiesel produced from WCO added with MWCNTs are blended with neat diesel that is discussed in this section. In the present research, biodiesel produced from WCO added with a different fraction of MWCNTs. Further, the model's accuracy is evaluated via regression analysis. The correlation

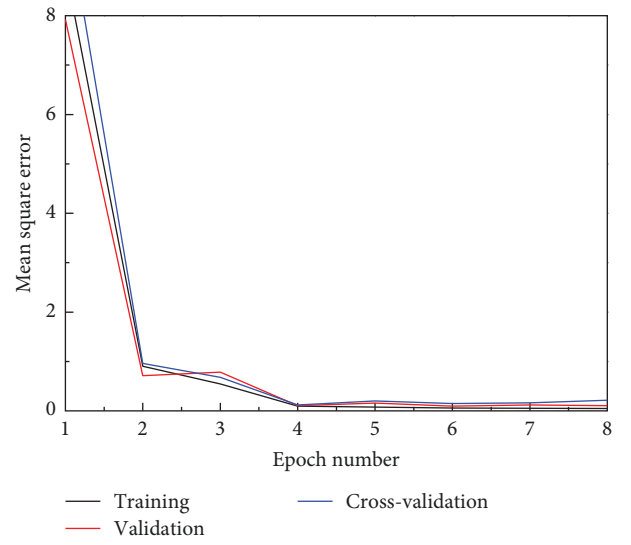

Figure 17: Optimum performance of multilayer neural network.

Table 8: MSE values for different hidden neurons.

S. No.	Outputs/targets	Topology	MSE validation
1.	HC, CO, and NO_x	3_2 Hidden_3	0.175
2.	HC, CO, and NO_x	3_4 Hidden_3	0.135
3.	HC, CO, and NO_x	3_6 Hidden_3	0.113
4.	HC, CO, and NO_x	3_8 Hidden_3	0.102
5.	HC, CO, and NO_x	3_10 Hidden_3	0.095
6.	HC, CO and NO_x	3_12 Hidden_3	0.243

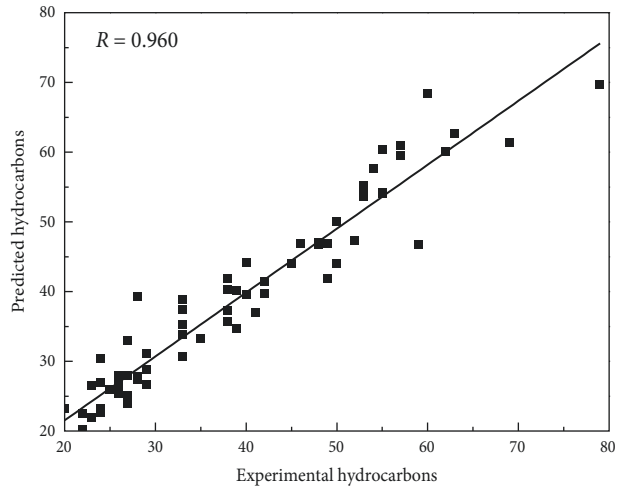

Figure 18: Experimental and predicted hydrocarbons values for all test conditions.

coefficient (R) criterion is employed for the measurement of model's accuracy. The "R" indicates the correlation between predicted and experimental values. The experimental and predicted emissions are compared for all test conditions. The experimental and MLNN-model-predicted emission characteristics are shown in Figures 18–20. These figures indicate the MLNN model accurately as its "R" values are

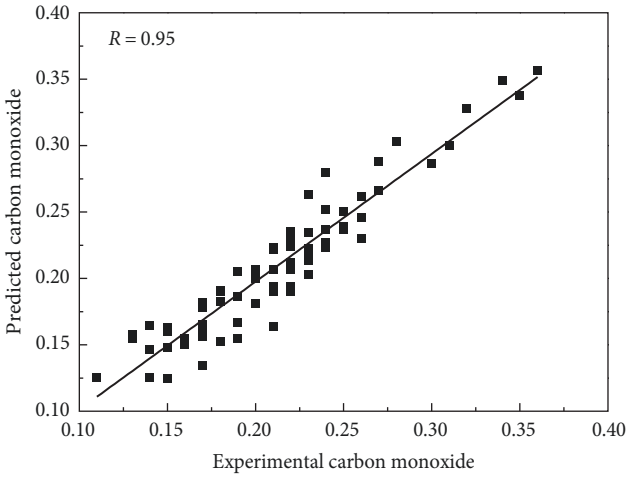

Figure 19: Experimental and predicted carbon monoxide values for all test conditions.

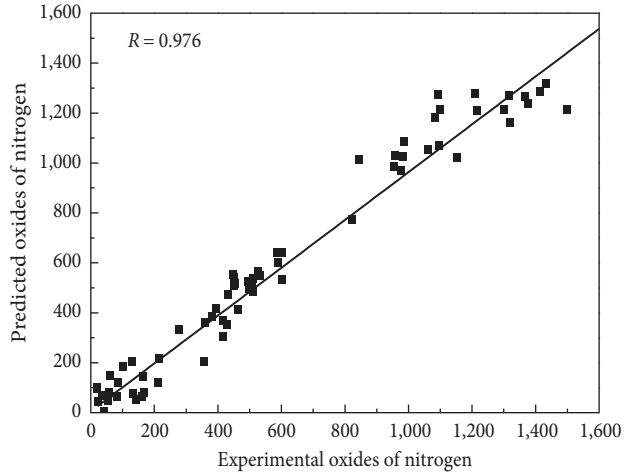

Figure 20: Experimental and predicted oxides of nitrogen values for all test conditions.

0.96, 0.95, and 0.98 for HC, CO, and NO_x, respectively. It further shows that the MLNN model is efficient in predicting emissions of tested engine with reasonable accuracy. Further, the relative error RE between experimental and predicted values is described using Equation (5).

$$\mathrm{RE} = \frac{|Y_{\text{predicted}} - Y_{\text{experimental}}|}{Y_{\text{experimental}}} \times 100, \tag{5}$$

where $Y_{\text{experinental}}$ and $Y_{\text{predicted}}$ are experimental and predicted values, respectively.

Thereafter, the values of *RE* are average of all test conditions. The prediction ability of the model for all test conditions of the engine is measured using averaged RE and *R* between experimental and predicted HC, CO, and NO_x values for all test conditions (Table 9).

Table 9: Performance of the model.

Emissions	Averaged relative error (%)	*R*
HC	0.83	0.96
CO	1.01	0.95
NO_x	1.05	0.976

5. Conclusions

In this manuscript, the use of the MLNN model for the prediction of HC, CO, and NO_x from a four-stroke single-cylinder CI engine runs on WCO biodiesel added with MWCNTs has been investigated. The MLNN model developed in this work uses a backpropagation algorithm. The optimum structure 3-10-3 is chosen for emission prediction at any given test conditions of engine as it denotes the MSE equal to 0.095. Further, the prediction ability of the model for all test conditions of the engine is measured using averaged RE and correlation coefficient (*R*). The average *RE* between experimental and predicted HC, CO, and NO_x values is found to be 0.83%, 1.01%, and 1.05%, respectively. The "*R*" between experimental and predicted HC, CO, and NO_x are also given in Figures 18–20, and are found to be 0.96, 0.95, and 0.976, respectively. The results indicate that values predicted from MLNN and the experiments are close to one another. Furthermore, the comparison of experimental results and MLNN predicts shows that CI/diesel engines run on WCO biodiesel dispersed with MWCNTs can be correctly modeled through MLNN. Therefore, the use of MLNN is appropriate for predicting the emissions of the CI engine, minimizing the cost, time, and labor effort. Additionally, the model can also be fit into the controller.

Data Availability

All the data used to support the findings of this study are included within the article.

Conflicts of Interest

The authors declare that they have no conflicts of interest.

Authors' Contributions

All authors contributed equally in the preparation of the manuscript.

Funding

The work has been financially supported by Vision Group on Science and Technology (VGST), Bengaluru 560001, Karnataka, India through Research Grant for Scientist/Faculty (RGS/F) Scheme (Letter No. KSTePS/VGST/RGS-F/GRDNo. 980/2020-21/104 dated 26/08/2021).

References

[1] S. P. Singh and D. Singh, "Biodiesel production through the use of different sources and characterization of oils and their

esters as the substitute of diesel: a review," *Renewable and Sustainable Energy Reviews*, vol. 14, no. 1, pp. 200–216, 2010.

[2] J. Hwang, Y. Jung, and C. Bae, "Spray and combustion of waste cooking oil biodiesel in a compression-ignition engine," *International Journal of Engine Research*, vol. 16, no. 5, pp. 664–679, 2015.

[3] A. Talebian-Kiakalaieh, N. A. Amin, and H. Mazaheri, "A review on novel processes of biodiesel production from waste cooking oil," *Applied Energy*, vol. 104, pp. 683–710, 2013.

[4] M. G. Kulkarni and A. K. Dalai, "Waste cooking oil-an economical source for biodiesel: a review," *Industrial & Engineering Chemistry Research*, vol. 45, no. 9, pp. 2901–2913, 2006.

[5] S. A. Ali, S. Hunagund, S. S. Hussain, and A. H. Bagwan, "The effect of nanoparticles dispersed in waste cooking oil (WCO) biodiesel on thermal performance characteristics of VCR engine," *Materials Today: Proceedings*, vol. 43, Part 2, pp. 888–891, 2020.

[6] M. Kareemullah, A. Afzal, K. Fazlur Rehman, K. Shahapurkar, H. Khan, and N. Akram, "Performance and emission analysis of compression ignition engine using biodiesels from acid oil, mahua oil, and castor oil," *Heat Transfer*, vol. 49, no. 2, pp. 858–871, 2020.

[7] T. N. Verma, U. Rajak, A. Dasore et al., "Experimental and empirical investigation of a CI engine fuelled with blends of diesel and roselle biodiesel," *Scientific Reports*, vol. 11, Article ID 18865, 2021.

[8] K. Nantha Gopal, A. Pal, S. Sharma, C. Samanchi, K. Sathyanarayanan, and T. Elango, "Investigation of emissions and combustion characteristics of a CI engine fueled with waste cooking oil methyl ester and diesel blends," *Alexandria Engineering Journal*, vol. 53, no. 2, pp. 281–287, 2014.

[9] M. A. Lenin, M. R. Swaminathan, and G. Kumaresan, "Performance and emission characteristics of a DI diesel engine with a nano fuel additive," *Fuel*, vol. 109, pp. 362–365, 2013.

[10] R. N. Mehta, M. Chakraborty, and P. A. Parikh, "Nanofuels: combustion, engine performance and emissions," *Fuel*, vol. 120, pp. 91–97, 2014.

[11] S. S. Kumar, K. Rajan, V. Mohanvel et al., "Combustion, performance, and emission behaviors of biodiesel fueled diesel engine with the impact of alumina nanoparticle as an additive," *Sustainability*, vol. 13, no. 21, Article ID 12103, 2021.

[12] S. Mukhopadhyay, A. Malhotra, N. Choudhary, and N. Kumar, "Experimental investigations of metal oxide nano-additives on working characteristics of CI engine," SAE Technical Paper 2019-01-0794, 2019.

[13] U. Ağbulut, M. Karagöz, S. Sarıdemir, and A. Öztürk, "Impact of various metal-oxide based nanoparticles and biodiesel blends on the combustion, performance, emission, vibration and noise characteristics of a CI engine," *Fuel*, vol. 270, Article ID 117521, 2020.

[14] U. Rajak, U. Ağbulut, I. Veza, A. Dasore, S. Sarıdemir, and T. N. Verma, "Numerical and experimental investigation of CI engine behaviours supported by zinc oxide nanomaterial along with diesel fuel," *Energy*, vol. 239, Part E, Article ID 122424, 2022.

[15] M. Hawi, A. Elwardany, M. Ismail, and M. Ahmed, "Experimental investigation on performance of a compression ignition engine fueled with waste cooking oil biodiesel-diesel blend enhanced with iron-doped cerium oxide nanoparticles," *Energies*, vol. 12, no. 5, Article ID 798, 2019.

[16] P. Tewari, E. Doijode, N. R. Banapurmath, and V. S. Yaliwal, "Experimental investigation on a diesel engine fuelled with multi walled carbon nano tubes blended biodiesel fuels," *International Journal of Emerging Technology and Advanced Engineering*, vol. 3, pp. 72–76, 2013.

[17] J. S. Basha and R. B. Anand, "An experimental investigation in a diesel engine using carbon nano tubes blended water-diesel emulsion fuel," *Proceedings of the Institution of Mechanical Engineers, Part A: Journal of Power and Energy*, vol. 225, no. 3, pp. 279–288, 2011.

[18] A. Prabhu, "Nanoparticles as additive in biodiesel on the working charecteristics of a DI diesel engine," *Ain Shams Engineering Journal*, vol. 9, no. 4, pp. 2343–2349, 2018.

[19] A. Ranjan, S. S. Dawna, J. Jayaprabakar, N. Nirmala, K. Saikiran, and S. Sai Sriram, "Experimental investigation on effect of MgO nanoparticles on cold flow properties, performance, emission and combustion characteristics of waste cooking oil biodiesel," *Fuel*, vol. 220, pp. 780–791, 2018.

[20] J. I. Ramos, *Internal Combustion Engine Modeling*, Hemisphere Publishing Corporation, Washington DC, 1989.

[21] S. A. Ali and S. Saraswati, "A comparison of sliding mode and FRF based observers for cylinder pressure estimation of SI engine," *Transactions of the Institute of Measurement and Control*, vol. 39, no. 2, pp. 163–172, 2017.

[22] T. F. Yusaf, D. R. Buttsworth, K. H. Saleh, and B. F. Yousif, "CNG-diesel engine performance and exhaust emission analysis with the aid of artificial neural network," *Applied Energy*, vol. 87, no. 5, pp. 1661–1669, 2010.

[23] B. R. Hosamani, S. A. Ali, and V. Katti, "Assessment of performance and exhaust emission quality of different compression ratio engine using two biodiesel mixture: artificial neural network approach," *Alexandria Engineering Journal*, vol. 60, no. 1, pp. 837–844, 2021.

[24] Z. Said, P. Sharma, L. Syam Sundar, A. Afzal, and C. Li, "Synthesis, stability, thermophysical properties and AI approach for predictive modelling of Fe_3O_4 coated MWCNT hybrid nanofluids," *Journal of Molecular Liquids*, vol. 340, Article ID 117291, 2021.

[25] P. V. Elumalai, R. Krishna Moorthy, M. Parthasarathy et al., "Artificial neural networks model for predicting the behavior of different injection pressure characteristics powered by blend of biofuel-nano emulsion," *Energy Science & Engineering*, vol. 10, no. 7, pp. 2367–2396, 2022.

[26] S. H. Hosseini, A. Taghizadeh-Alisaraei, B. Ghobadian, and A. Abbaszadeh-Mayvan, "Artificial neural network modelling of performance, emission, and vibration of CI engine using alumina nano-catalyst added to diesel-biodiesel blends," *Renewable Energy*, vol. 149, pp. 951–961, 2020.

[27] S. F. Arbadali, B. Najafi, M. Aghbashlo, Z. Khaunanai, and M. Tabatabaei, "Performance and emission analysis of a dual-fuel engine operating on high natural gas substitution rates ignited by aqueous carbon nanoparticles-laden diesel/biodiesel emulsions," *Fuel*, vol. 294, Article ID 120246, 2021.

[28] M. Norgaard, O. Ravn, N. K. Poulsen, and L. K. Hansen, *Neural Networks for Modelling and Control of Dynamic Systems*, Springer, 2000.

[29] S. Haykin, *Neural Networks: A Comprehensive Foundation*, Pearson Education Inc., 2002.